



HAL
open science

Compact and efficient injection of light into band-edge slow-modes

Philippe Velha, Jean-Paul Hugonin, Philippe Lalanne

► **To cite this version:**

Philippe Velha, Jean-Paul Hugonin, Philippe Lalanne. Compact and efficient injection of light into band-edge slow-modes. *Optics Express*, 2007, 15 (10), pp.6102-6112. hal-00846685

HAL Id: hal-00846685

<https://hal-iogs.archives-ouvertes.fr/hal-00846685>

Submitted on 19 Jul 2013

HAL is a multi-disciplinary open access archive for the deposit and dissemination of scientific research documents, whether they are published or not. The documents may come from teaching and research institutions in France or abroad, or from public or private research centers.

L'archive ouverte pluridisciplinaire **HAL**, est destinée au dépôt et à la diffusion de documents scientifiques de niveau recherche, publiés ou non, émanant des établissements d'enseignement et de recherche français ou étrangers, des laboratoires publics ou privés.

Compact and efficient injection of light into band-edge slow-modes

P. Velha, J. P. Hugonin, and P. Lalanne*

Laboratoire Charles Fabry de l'Institut d'Optique, CNRS, Univ Paris-Sud, Campus Polytechnique, RD 128
91127 Palaiseau Cedex, France.

*Corresponding author : philippe.lalanne@institutoptique.fr

Abstract: We design compact (a few wavelength long) and efficient (>99%) injectors for coupling light into slow Bloch modes of periodic thin film stacks and of periodic slab waveguides. The study includes the derivation of closed-form expressions for the injection efficiency as a function of the group-velocity of injected light, and the proof that 100% coupling efficiencies for arbitrary small group velocities is possible with an injector length scaling as $\log(c/v_g)$. The trade-off between the injector bandwidth and the group velocity of the injected light is also considered.

©2007 Optical Society of America

OCIS codes: (130.2790) Guided waves; (260.2110) Electromagnetic theory; (350.7420) Waves; (999.9999) slow modes; (999.9999) Group-velocity impedance mismatch; (999.9999) Periodic waveguides.

References and links

1. S. E. Harris, "Electromagnetically induced transparency," *Phys. Today* **50**, 36-42 (July 1997).
2. J. Khurgin, "Expanding the bandwidth of slow-light photonic devices based on coupled resonators," *Opt. Lett.* **30**, 2778-2780 (2005).
3. J. Poon, L. Zhu, G. DeRose, and A. Yariv, "Transmission and group delay of microring coupled-resonator optical waveguides," *Opt. Lett.* **31**, 456-458 (2006).
4. M. F. Yanik and S. Fan, "Stopping light all optically," *Phys. Rev. Lett.* **92**, 083901 (2004).
5. M. Notomi, A. Shinya, S. Mitsugi, G. Kira, E. Kuramochi and T. Tanabe "Optical bistable switching action of Si high-Q photonic-crystal nanocavities," *Opt. Express* **13**, 2678-2687 (2005).
6. A. Yu. Petrov and M. Eich, "Zero dispersion at small group velocities in photonic crystal waveguides," *Appl. Phys. Lett.* **85**, 4866-4868 (2004).
7. D. Mori and T. Baba, "Wideband and low dispersion slow light by chirped photonic crystal coupled waveguide," *Opt. Express* **13**, 9398-9408 (2005).
8. T. F. Krauss, "Photonic Crystals shine on," *Phys. World* 32-36, (February 2006).
9. A. Melloni, F. Morichetti, and M. Martinelli, "Linear and Nonlinear propagation in coupled resonator slow-wave optical structures," *Opt. Quantum Electron.* **35**, 365-379 (2003).
10. G. Lenz, B. J. Eggleton, C. K. Madsen, and R. E. Slusher, "Optical delay lines based on optical filters," *IEEE J. Quantum Electronics* **37**, 525-532 (2001).
11. Y. A. Vlasov and S. J. McNab, "Coupling into the slow light mode in slab-type photonic crystal waveguides," *Opt. Lett.* **31**, 50-52 (2006).
12. M. Povinelli, S. Johnson, and J. Joannopoulos, "Slow-light, band-edge waveguides for tuneable time delays," *Opt. Express* **13**, 7145-7159 (2005).
13. J. P. Hugonin and P. Lalanne, "Perfectly-matched-layers as nonlinear coordinate transforms: a generalized formalization," *J. Opt. Soc. Am. A.* **22**, 1844-1849 (2005).
14. P. Yeh, *Optical waves in layered media*, (J. Wiley and Sons, New York 1988).
15. J. M. Bendickson, J. P. Dowling, and M. Scalora, "Analytic expressions for the electromagnetic mode density in finite, one-dimensional, photonic band-gap structure," *Phys. Rev. E* **53**, 4107-4121 (1996).
16. H. A. Haus, *Waves and fields in optoelectronics* (Prentice-Hall International, London, 1984).
17. K. Sakoda, *Optical properties of photonic crystals*, (Springer-Verlag, Berlin 2001) Chap. 11.
18. B. Momeni and A. Adibi, "Adiabatic stage for coupling of light to extended Bloch modes of photonic crystal," *Appl. Phys. Lett.* **87**, 171104 (2005).
19. L. A. Coldren and S. W. Corzine, *Diode lasers and photonic integrated circuits*, (J. Wiley and Sons, New York, 1995).
20. C. Sauvan, G. Lecamp, P. Lalanne, and J. P. Hugonin, "Modal-reflectivity enhancement by geometry tuning in photonic crystal microcavities," *Opt. Exp.* **13**, 245-255 (2005).

21. P. Lalanne and J. P. Hugonin, "Bloch-wave engineering for high Q's, small V's microcavities," *IEEE J. Quantum Electron.* **39**, 1430-1438 (2003).
22. J. C. Lagarias, J. A. Reeds, M. H. Wright, and P. E. Wright, "Convergence properties of the Nelder-Mead Simplex Method in Low Dimensions," *SIAM J. Optim.* **9**, 112-147 (1998).
23. D. Gerace and L. C. Andreani, "Effects of disorder on propagation losses and cavity Q-factors in photonic crystal slabs," *Photonics and Nanostructures-fundamentals and applications* **3**, 120-128 (2005).
24. E. Kuramochi, M. Notomi, S. Hughes, A. Shinya, T. Watanabe, and L. Ramunno, "Disorder-induced scattering loss of line-defect waveguides in photonic crystal slabs," *Phys. Rev. B* **72**, 161318 (2005).
25. M. D. Settle, R. J. P. Engelen, M. Salib, A. Michaeli, L. Kuipers, and T. F. Krauss, "Flatband slow light in photonic crystals featuring spatial pulse compression and terahertz bandwidth," *Opt. Express* **15**, 219-226 (2007).
26. H. A. Macleod, *Thin-film optical filters*, (Adam Hilger LTD, London 1969).
27. R. E. Collin, *Field theory of guided waves*, (London, Section 9 1960).

1. Introduction

In recent years, faster optical telecommunication and data processing have motivated research towards solutions to try to minimize the involvement of electronics in signal manipulation and to keep signals in the optical domain as long as possible. For true all-optical signal processing, one has to use optical non-linearities. Unfortunately, these non-linearities are extremely weak, thus requiring large interaction lengths or huge operational powers. Different approaches may be used to reinforce light-matter interactions including the elaboration of new materials [1] or of new structural geometries like coupled-resonator optical waveguides [2-3] or photonic-crystal (PC) microcavities [4-5]. In the quest for ultimate miniaturization, slow waves obtained by introducing a periodic corrugation along the z-axis of a waveguide appears as a promising approach [6-7]. Clearly, a crucial issue for integrated circuits using slow-wave waveguides is the realization of efficient light injectors between uniform z-invariant waveguides and slow-wave z-periodic waveguides.

Although it is indeed related to that of synthesizing apodized filters [8-10], the problem of designing efficient injectors has only been weakly addressed in the literature. Vlasov and his colleagues have experimentally investigated the impact of a fine variation of the termination of single-row defect PC waveguide [11]. The injection efficiency has been shown to depend on the exact shape of the termination, but efficient slow light couplings have not been observed. A natural approach for producing this crucial optical functionality consists in using adiabatic tapers that implement a progressive light slowdown through a continuous change of the waveguide geometry. This has been studied in Ref. [12] for periodic ridge waveguides incorporating teeth in the side of the waveguide. Remarkably efficient injectors with reflectivity as small as 0.001% have been designed with this approach, but this has been achieved with taper lengths of 50 periodicities and only for rather large group velocities close to $0.1c$. It can be easily shown that the length of tapers operating without any back-reflection in the taper sections (only forward-propagating Bloch modes are involved in the tapering process) rapidly increases as the group-velocity is reduced. Using a scaling factor of $(c/v_g)^3$ [12], it implies that such an approach would lead to taper lengths of ≈ 5000 periods for coupling light into a slow wave with $v_g=0.01c$.

In contrast, we hereafter consider slow-wave injectors that operate as interference filters (both backward and forward Bloch modes participate in the tapering process) and that can provide efficient injection in an ultra-compact way. Typically, we report on the design of efficient injectors with characteristic lengths of a few wavelengths. In Section 2, we start with the Bloch modes of periodic layers and analytically study the group-velocity impedance-mismatch problem arising at an interface between a uniform medium and a z-periodic layer stack. In particular we derive closed-form expression for the injection efficiency as a function of the group-velocity of injected light. This preliminary study is motivated by the fact that the injection problem is in essence one-dimensional and that simple intuitive analysis have not yet been presented for the back-reflection resulting at the interface between z-invariant and z-periodic media, despite its importance for our problem. Section 3 is devoted to the study of light injection at a single frequency. We show that injectors can be designed as simple Bragg

mirrors that allows 100% coupling efficiencies for arbitrary small group velocities and that the injector length scales as $\log(c/v_g)$. In Section 4, we consider more realistic geometries composed of slits etched into a slab waveguide. Since radiation loss into the cladding is included into this problem, this geometry represents a test bed for even more realistic three-dimensional geometries, like PC waveguides, while preserving computational requirements at a moderate level. Using a combination of fully-vectorial methods [13] and of optimisation techniques, we design efficient and wavelength-long injectors that couple light into slow waves ($v_g/c=0.1-0.001$) with bandwidths of the order of 250 GHz at -1 dB. Section 5 summarizes the results.

2. Group-velocity impedance mismatch problem

We start with the scattering problem defined in Fig. 1(a). An incident plane wave in a uniform medium (refractive index n) is normally incident onto a semi-infinite periodic thin-film stack composed of lossless alternate layers with refractive indices n_H and n_L . Hereafter, we denote by a the periodicity constant of the thin film stack and by f (the fill factor) the fraction of material with refractive index n_H .

2.1 Injection efficiency

This scattering problem can be solved by considering the modes of the two semi-infinite media at a given frequency ω . We denote by $k = \omega/c$ the modulus of the free-space wave vector. The modes in the uniform medium are the forward- and backward-propagating plane waves, denoted $|P^+\rangle = \exp(jknz)$ and $|P^-\rangle = \exp(-jknz)$, with a unitary Poynting vector $|P^+\rangle = [E_x, H_y] = [(2/n)^{1/2}, (2n)^{1/2}]$ and $|P^-\rangle = [(2/n)^{1/2}, -(2n)^{1/2}]$. The modes of the periodic medium are the Bloch modes, $|B^+(z)\rangle = \exp(jkn_{\text{eff}} z)$ and $|B^-(z)\rangle = \exp(-jkn_{\text{eff}} z)$, with $|B^+\rangle$ and $|B^-\rangle$ two periodic functions of the z -coordinate and with n_{eff} the Bloch-mode effective index. $|B^+\rangle$ and $|B^-\rangle$ are calculated as the eigenstates of the unit-cell transfer matrix of the periodic medium and n_{eff} as the associated eigenvalues [14].

The bi-layer stack possesses a mirror-symmetry relatively to transversal planes in the layers of refractive index n_H , represented by the dashed vertical lines in Fig. 1(a) and located at planes $z=z_0+pa$, with p an integer. Similar planes exist for the layers of refractive index n_L . In every layer of the periodic structure, the functions $|B^+\rangle$ and $|B^-\rangle$ can be expanded as a superposition of two counter-propagative plane waves. We will denote by A_H and B_H , the modal coefficients of this decomposition in the transversal plane $z=z_0$, A_H referring to the forward plane wave and B_H to the backward plane wave. Thus, we have

$$|B^+(z=z_0+pa)\rangle = A_H |P^+\rangle + B_H |P^-\rangle, \quad (1)$$

The ratio $u=B_H/A_H$ between the backward- and forward-modal coefficients is an important parameter which describes the stationary character of the Bloch mode. Inside the photonic gap and at the band edges where $v_g=0$, $|u|=1$. Outside the photonic gap, u is real for lossless materials and using the analytical expressions obtained in [14-15], it can be further shown that

$$0 < u < 1, \quad (2a)$$

$$-1 < u < 0, \quad (2b)$$

for the valence and conduction bands, respectively. Similarly, the backward-propagating Bloch mode can be denoted by

$$|B^-(z=z_0+pa)\rangle = A'_H |P^+\rangle + B'_H |P^-\rangle, \quad (3)$$

Note that in general, there is no relation between $|B^-\rangle$ and $|B^+\rangle$, except if the periodic stack is composed of lossless materials or if it possesses a mirror-symmetry with respect to a transverse plane [15]. In this case, $B'_H=A_H$ and $A'_H=B_H$ showing that the u -factor of $|B^-\rangle$ is simply the inverse of that of $|B^+\rangle$ for the bi-layer stack.

After this few statements on Bloch modes, let us now go back to the scattering problem of Fig. 1(a). The total field in the uniform medium ($z < 0$) can be expressed as

$|P^+\rangle \exp(jknz) + r |P^-\rangle \exp(-jknz)$, where r is the modal reflectivity coefficient. Similarly, the field in the periodic medium is simply $t|B^+\rangle \exp(jkn_{\text{eff}}z)$, in the absence of illumination from the right side. By satisfying the boundary condition at $z = 0$ (continuity of E_y and H_x), one obtains

$$r = [(n-n_H) + u(n+n_H)\exp(j\phi)] / [(n+n_H) + u(n-n_H)\exp(j\phi)], \quad (4)$$

where $\phi = kn_H f a$ is the phase delay associated to the propagation through the layers with a refractive index n_H . The previous equation shows that the reflectance $|r|^2$ and the injection efficiency, equal to $T=1-|r|^2$ in the absence of loss, depend on Fresnel-type back-reflections through the ratio $(n-n_H)/(n+n_H)$, on the phase delay and on the u -factor of $|B^+\rangle$. Note that for $n=n_H$, r is simply given by $r=u \exp(j\phi)$ and the high reflectance $|r|^2$ close to the band-gap edges is purely due to the stationary character of $|B^+\rangle$ ($|u| \approx 1$). Using the 2x2 transfer-matrix formalism in Ref. [14], ϕ and u can be implicitly calculated as a function of the group-velocity v_g of $|B^+\rangle$. The injection efficiency $T=1-|r|^2$ (i.e. the coupling efficiency into $|B^+\rangle$), in the vicinity of the band-edges of the first valence and conduction bands, is shown in Fig. 1(b), for $0.1 < f < 0.9$.

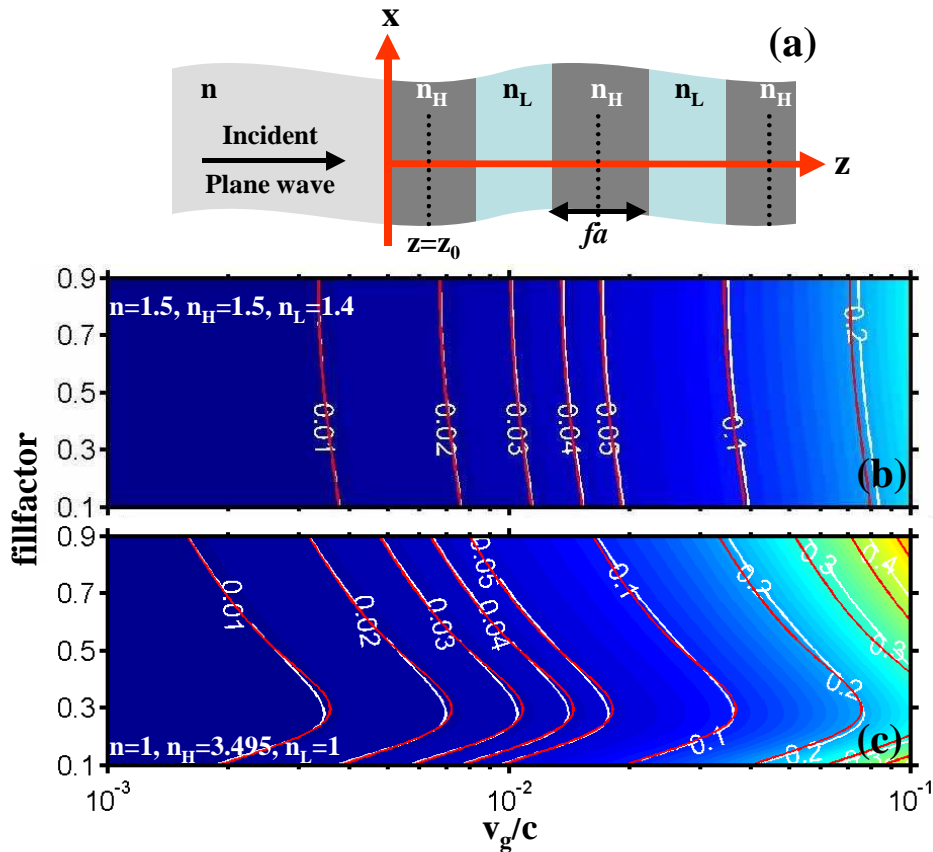


Fig. 1. Impedance mismatch problem. (a): Scattering at an interface between a uniform medium (refractive index n) and a semi-infinite bi-layer periodic stack (refractive indices n_H and n_L). (b) and (c): Injection efficiency T as a function of the group-velocity of the periodic-stack Bloch mode for different fill factors ($0.1 < f < 0.9$). Colormaps and white curves are exact numerical results obtained with the 2x2 transfer-matrix method in [14], and the superimposed solid-red curves are obtained using the approximate closed-form expressions. (b): data obtained in the vicinity of the valence band edge of a weak-modulation ($n_H=1.5$ and $n_L=1.4$) stack for $n=n_H$. (c): data obtained in the vicinity of the conduction band edge of a strong-modulation stack ($n_H=3.495$ and $n_L=1$) for $n=n_L$.

2.2 Approximate closed-form expression for the injection efficiency

In order to get a better insight into the group-velocity impedance mismatch illustrated in Fig. 1(b), it is important to have at one's disposal simple expressions for the reflectance as a function of the v_g for the different optical (n , n_H and n_L) and geometrical (f) parameters of the problem. According to Eq. (5), one needs to express $u=A_H/B_H$ and ϕ as a function of v_g . For that purpose, we use the fact that v_g is the velocity of the energy propagation, $v_g=aP/\mathcal{E}_m$, with P the power flow and with $\mathcal{E}_m=1/2 \int_{\text{Cell}} \epsilon(z) |E(z)|^2 dz$, a quantity related to the mode volume of B^+ . P is simply equal to $|A_H|^2 - |B_H|^2$ and \mathcal{E}_m can be expressed as a function of A_H and B_H . We do not repeat the lengthy calculation here (a copy of a hand-written derivation could be provided on request), and we obtain for a bi-layer system

$$(v_g/c) [\alpha(1+u^2)+2\beta u] = 2n_H(1-u^2), \quad (5)$$

with $\alpha=(1+f)n_H^2+(1-f)n_L^2$ and $\beta=(1-f)\cos(\phi)(n_H^2-n_L^2)$. Equation (5) is exact and provides a general relationship between the free-space wavevector k (β depends on k through ϕ), the group velocity v_g and the stationary ratio u . To express ϕ as a function of v_g , one may expand it in a power series of v_g/c , $\phi=\phi^{(0)}+O(v_g/c)$, and by retaining only the first term $\phi^{(0)}$, Eq. (5) can be solved for $u(v_g)$

$$u_{VB} = 1 - \left(\frac{\alpha + \beta_{VB}}{2n_H} \right) v_g/c + O(v_g/c)^2, \quad \text{and} \quad (6a)$$

$$u_{CB} = -1 + \left(\frac{\alpha - \beta_{CB}}{2n_H} \right) v_g/c + O(v_g/c)^2, \quad (6b)$$

where β_{VB} and β_{CB} correspond to $\beta(\phi=\phi^{(0)})$ at the valence and conduction band edges, respectively. For quarter-wave periodic stacks, $f=(1+n_H/n_L)^{-1}$, a closed-form expression for the phase delay $\phi^{(0)}$ exists [14], $\phi^{(0)} = \pi/2 \pm \text{asin}\left(\frac{n_H - n_L}{n_H + n_L}\right)$, the plus and minus signs holding for the conduction and valence bands. However for arbitrary f values, the calculation of $\phi^{(0)}$ requires to solve for a transcendental equation, see Section 6.2 in Ref. [14]. To retrieve full analyticity, one may use the classical coupled-wave method [16], assuming that the Bloch modes of the periodic media is described by only two counter-propagative slowly-varying z -functions that are coupled at the band edges by the first-Fourier coefficient of the relative-permittivity modulation, $\epsilon_1=(n_H^2-n_L^2)f \text{sinc}(\pi f)$. Within this approach that is all the more accurate as n_H-n_L is small, we have

$$\phi^{(0)} \approx \pi f n_H [1 \pm \epsilon_1 / (2\epsilon_0)] / \epsilon_0^{1/2}, \quad (7)$$

where $\epsilon_0=f n_H^2+(1-f)n_L^2$ is the DC-component of the Fourier coefficients of the relative permittivity, the plus and minus signs holding for the conduction and valence bands. By substituting Eqs. (7) and (6) into Eq. (4), one easily obtains a closed-form expression for the injection efficiency $T=1-|r|^2$ as a function of the dielectric material properties n_H , n_L and n and of the fill factor f in the limit of small group velocities. As noted before, for $n=n_H$, the expressions largely simplifies and one obtains

$$T_{VB} = \left(\frac{\alpha + \beta_{VB}}{n_H} \right) v_g/c, \quad T_{CB} = \left(\frac{\alpha - \beta_{CB}}{n_H} \right) v_g/c. \quad (8)$$

The predictions of the coupled-wave model are shown by the superimposed solid-red curves in Figs. 1(b) and 1(c) for a low- and high-index contrasts, respectively. Despite the large refractive-index modulation used in Fig. 1(c), which is likely not to be accurately described by the two-first Fourier coefficients of the relative permittivity, the agreement with

the transfer-matrix results is quantitative. As we checked with computational results obtained by solving the transcendental equation for the phase delay $\phi^{(0)}$ at the band edges, the deviation in Figs. 1(b) and 1(c) mainly results from the coupled-wave-method approximation used to derive Eq. (7).

For small-index contrasts, β is much smaller than α , and the injection efficiencies in Eq. (8) are almost identical, $T_{VB} \approx T_{CB}$. Additionally, since $\alpha \approx n_H^2 + n_L^2$, the injection efficiency weakly depends on f , as illustrated in Fig. 1(b). For large index contrasts, β cannot be neglected and for $n \neq n_H$, Eq. (4) instead of Eq. (8) has to be used. Both situations result in a dependence of the injection efficiency with the fill factor through the phase delay ϕ in Eq. (4) or directly through the coefficients α and β . This is illustrated in Fig. 1(c), which holds for $n_H/n_L = 3.495$ and for $n \neq n_H$.

Finally, note that the expressions in Eq. (8) largely differ from the usual ansatz [17-18], $r = (v_{g1} - v_{g2}) / (v_{g1} + v_{g2})$, where v_{g1} and v_{g2} are the group-velocities of the incident and transmitted waves. For $v_{g2} \ll v_{g1}$, the ansatz, which leads to $T = 4v_{g2}/v_{g1}$, completely ignores the difference of injection efficiencies at the two band edges, which is predicted by the transfer-matrix computational results or by the approximate formula of Eq. (8).

3. Slow-mode injectors

The group-velocity impedance mismatch problem illustrated in Fig. 1 evidences the necessity of designing injectors for efficiently coupling light into slow modes. Indeed injectors are crucial for successful implementation or characterisation of systems relying on slow-mode field enhancements. In this Section, we show that, by engineering the interface between the uniform medium and the periodic stack, injectors with very-short length can be designed even for small group velocities. This result is established for 1D thin-film stacks and 2D periodic waveguides composed of slits in a slab waveguide.

3.1 Perfect injection in 1D thin-film stacks

We start with one-dimensional problems like in the previous section and we consider the geometry shown in Fig. 2(a), where a thin film stack (the injector to be further designed) is inserted between a uniform medium and a periodic stack supporting slow modes at the band edges. In Fig. 2(b), we sketch a situation corresponding to perfect injection. Under illumination from the uniform medium with an unit-amplitude incident normalized plane wave, no light is back reflected at plane S_1 and all the incident power is coupled into the forward-propagating slow Bloch mode of the periodic stack. This slow Bloch mode $|B^+\rangle = \exp(jk n_{\text{eff}} z)$ is defined at plane S_2 by its forward and backward-modal coefficients, A_H and B_H , with $|A_H| \approx |B_H| \gg 1$ in the slow-mode regime and with $|A_H|^2 - |B_H|^2 = 1$ for the sake of normalization. Perfect injection is achieved if $|t| = 1$, t being the complex amplitude injection coefficient.

Although the following derivation can be straightforwardly obtained using time-reversal properties of lossless thin film stacks [15], we aim at a more general derivation hereafter, and we rather invoke reciprocity arguments that remain valid even for situations potentially encompassing out-of-plane scattering, as in periodic waveguides for instance. We additionally drop off any argument related to the existence of mirror-symmetry planes. Figure 2(c) depicts a reciprocal problem, where the backward-propagating Bloch mode $|B^-\rangle = \exp(-jk n_{\text{eff}} z)$ impinging from the periodic stack onto the injector transmits light into the backward-propagating plane wave $|P^-\rangle = \exp(-jk n z)$ at plane S_1 , with a complex transmission coefficient t . We denote by A'_H and B'_H its forward and backward-modal coefficients, and since the backward-propagating Bloch mode in (c) possesses the same group velocity as the forward-propagating Bloch mode in (b), $|A'_H| \approx |B'_H| \gg 1$ in the slow-mode regime. Indeed solving the synthesis problem of Fig. 2(b) is identical to solving that of Fig. 2(c). As shown now, solving the synthesis problem in (c) can be done in an intuitive way.

For perfect injection in (b) guaranties that $|t|=1$ in (c). Thus, no light is back reflected into the forward-propagating Bloch mode $|B^+\rangle$ in (c) and all waves are shown in (c). Since $|A'_H| \approx |B'_H| \gg 1$ with $|B'_H| > |A'_H|$, Fig. 2(c) evidences that the injector basically acts as a mirror for the plane waves, which reflects most of the light with a modal reflectivity coefficient $r_m = A'_H/B'_H$ and which transmits light with a modal transmission $|t/B'_H|^2 = 1 - |r_m|^2$. Thus, designing an injector to couple light into a slow mode amounts to synthesize a mirror. In fact, the smaller the group velocity, the larger the mirror reflectance is. Figure 2(d) shows the general solution of the synthesis problem. The injector is composed of a mirror with reflectance $|A'_H/B'_H|^2$ and eventually of a phase plate, the latter being used to guaranty that the argument of r_m strictly matches the argument of the stationary-ratio (A'_H/B'_H) of the backward-propagating Bloch mode $|B^-\rangle$.

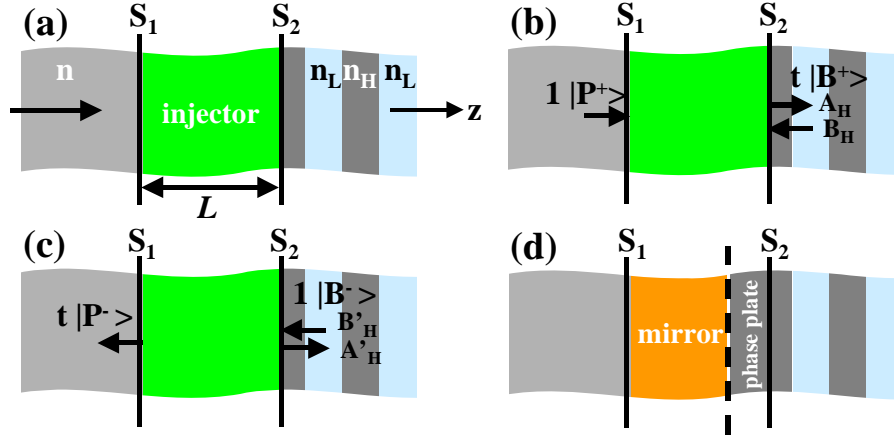


Fig. 2. A slow-mode injector at a single frequency is basically a mirror. (a) Definition of the injector parameters : length L , interface S_1 between the coupler and the uniform medium and interface S_2 between the coupler and the periodic stack supporting a slow Bloch mode. (b) Perfect injector at a single frequency for a plane wave incident from the uniform medium. (c) Reciprocal problem. The incident illumination is the reciprocal Bloch mode propagating towards the negative z -direction. (d) General solution of the synthesis problem : the injector is composed of a mirror and of a phase plate.

Thus, perfect injection into a slow Bloch mode at a single frequency $\omega/c=2\pi/\lambda$ is made possible with a mirror, and this for arbitrary small group velocities. For a mirror designed as a quarter-wave stack at the frequency ω , closed-form expressions for the modal reflection coefficient r_m are available as a function of the number m of alternate layer pairs. For a mirror form with the same materials as the periodic stack, it is shown [19] that $r_m = (1 - (n_L/n_H)^{2m}) / (1 + (n_L/n_H)^{2m})$, which is approximately equal to $1 - 2(n_L/n_H)^{2m}$ for large m . By equating the latter expression with the stationary-ratio defined by Eqs. (6a) or (6b), we obtain that $(n_L/n_H)^{2m} = \left(\frac{\alpha - \beta}{4n_H} \right) v_g/c$, where β holds for β_{VB} or β_{CB} . Therefore, the injector length L scales as the logarithm of c/v_g and we have

$$L = g\lambda \log(c/v_g), \quad (9)$$

with g a constant parameter that depends on n , n_L , n_H and f . The length in Eq. (9) largely contrasts with those obtained with an adiabatic approach. To check this, we have solved the scattering problem shown in Fig. 2(a) with the 2×2 transfer-matrix formalism [14], for a bi-layer periodic stack with $n_H=3.495$, $n_L=1$ and $f=0.5$. The injectors are simply quarter-wave Bragg mirrors composed of alternated layers with the same refractive indices n_H and n_L , and designed at a Bragg wavelength corresponding to the band edge of the periodic stack. Figure 3 shows the transmission T into the slow Bloch mode of the periodic stack, as a function of the

frequency of the incident plane wave (actually v_g on the horizontal axis). The different curves are obtained for different m values, ranging from $m=1$ to $m=5$. They have been calculated in the vicinity of the first valence band, but almost identical curves have been obtained for the conduction band. As expected, perfect injection ($T=1$) is achieved in all cases. Additionally we note that the group velocities corresponding to $T=1$ scale linearly with m (in log scale), as predicted by Eq. (9). The horizontal arrows delimitate the 1dB ($T=0.8$) bandwidth of the injector in GHz. Indeed the bandwidth vanishes as $(v_g)^2$, and for very small group velocities of $\approx 10^{-4}$, it is actually very small, $\approx 10^{-2}$ GHz. Therefore, injectors designed as pure mirrors cannot be used for full-optical signal processing applications, but they may find applications for single frequency applications and may be incorporated into new architectures in DBR and DFB lasers for instance.

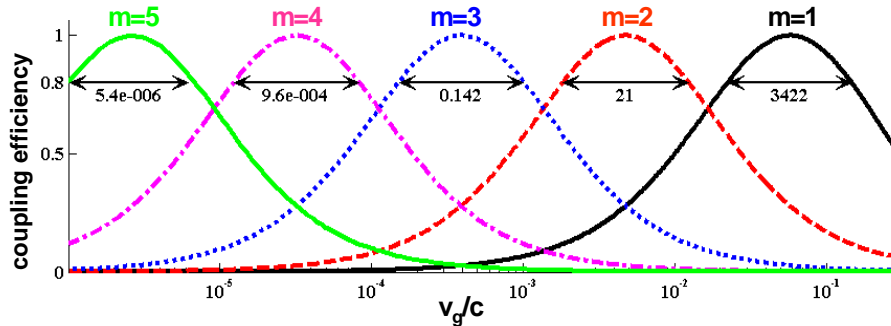


Fig. 3. Coupling efficiency into the slow-mode of a periodic stack (n_H, n_L) as a function of the group velocity (log scale) of the slow mode. Different injectors are considered. They are all composed of Bragg mirrors (n_H, n_L) with an increasing number of repeated pairs, $m=1, \dots, 5$. The results are obtained in the vicinity of the valence band edge of the periodic stack. The horizontal arrows indicate the bandwidths in GHz of the different injectors for $T=0.8$ (-1dB).

3.2 Broadband injection in 2D periodic waveguides

So far, we have only considered thin-film-stack geometries and injectors operating at a single frequency. In planar integrated systems, the out-of-plane scattering into the claddings is an important point of concern that cannot be inferred from 1D calculations. The transverse mode-profile mismatch between the mirror evanescent Bloch mode, the guided mode of the z -invariant waveguide and the slow Bloch mode of the periodic waveguide, is expected to lower the mirror reflectance [20]. Thus according to the previous analysis, this loss should prevent injection at small group velocities, since the latter requires very high reflectance. However, we believe that mirrors that incorporate tapers on both extremities [21] may allow reducing the mismatch and in turns may be used for efficient injection even at very small group velocities. We believe that by combining the mirror-design procedure in Refs. [20-21] and the 1D analysis of Section 3.1, tapered mirrors with very high injection efficiencies can be designed for a single frequency, even for small group velocities. This will be illustrated by the results discussed below. Another more specific problem in the present context is the design of injectors that achieve a bandwidth broad enough to support high data-rate telecommunication signals, while maintaining the losses at a small level. For that important problem, the 1D analysis of Section 3.1 performed at a single frequency does not help much, and this is the reason why we will rely on numerical optimisation techniques in the following example.

In order to study the feasibility of such injectors with relatively broadband and lossless couplings, we consider a semi-infinite periodic waveguide composed of a silicon (refractive index 3.5) 260-nm thick core with air claddings. Above $\lambda = 1.5 \mu\text{m}$, the waveguide supports a single TE guided mode. The periodic waveguide has a period $a=350 \text{ nm}$ and is composed of 185-nm large lamellar grooves etched down to the SiO_2 substrate. Because of the low cladding refractive indices, the periodic waveguide supports a single truly-guided slow-mode

in the vicinity of the band edge ($k \approx \pi/a$) of the first valence and conduction bands. For broadband and lossless couplings, we have optimised injectors consisting of five slits and five ridges fully etched through the waveguide core, the free parameters being the lengths of the ridges and grooves. An example of an optimised structure is shown in Fig. 4(a). For the optimisation we use the simplex search Nelder-Mead method. This direct method that does not use numerical or analytic gradients relies on an iterative simplex-minimization approach that progressively reduces the explored volume in the parameter hyper-space [22]. The function value used for the optimisation is the weighted sum of the injector efficiency calculated for five different wavelengths in the close vicinity of a central wavelength corresponding to a targeted small group velocity of the periodic waveguide. In addition, we have imposed a firm lower bound on the injection efficiency, $T > 99\%$ for the central wavelength.

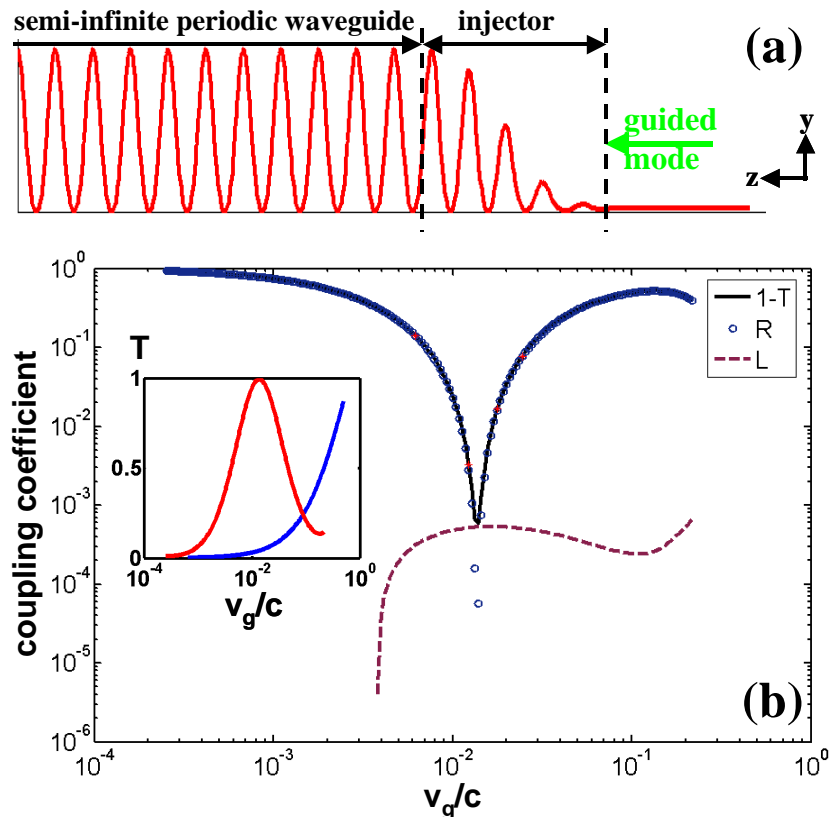


Fig. 4. Broadband injection from a planar waveguide to a periodic waveguide near the valence-band edge ($\lambda = 1.65 \mu\text{m}$). (a) Injector geometry optimized for coupling at $v_g/c \approx 0.01$. From left to right, the injector slit- and ridge-widths are 84, 143, 127, 158, 174 nm and 239, 213, 173, 166, 166 nm, respectively. The superimposed red curve represents the squared modulus of the transverse electric field at optimal coupling. (b) Performance of the injector predicted by fully vectorial computational results for the radiation loss L (dashed curve), the modal reflection R (blue circles) and the transmission T (actually $1-T$ is shown with a solid black curve). All quantities are displayed in a log scale. Inset: Injection efficiency T as a function of v_g with (red) and without (blue) injector. The maximum injection efficiency is as large as 0.999. In the absence of injector, this efficiency is only 0.25%.

Because of the strong corrugations, one needs to solve the Maxwell's equations with fully-vectorial theory for the optimisation. We have used an aperiodic Fourier Modal Method, based on an artificial periodization in the transverse direction with perfectly-matched layers at the boundary of the supercell [13]. Modal techniques are particularly efficient for performing

such optimisations because the integration along the z -direction is analytical. Once the eigenmodes of the two-layer system (waveguide and groove) are calculated for the five wavelengths, the optimisation just consists in searching the injector geometry by recursively computing the scattering matrices associated to various ridge and groove lengths. For the 2D injector-design problem (invariant along the slit y -axis) investigated in this work, very high accuracy (relative error below 0.1%) is achieved for the transmission, see details in Ref. [13].

As initial guesses for the optimisation, we have considered various Bragg mirrors with different groove and ridge lengths and different target group velocities. The optimisation has revealed that many different injector geometries can be used to inject light efficiently and that the most difficult criteria to fulfil is the broadband injection. Although the parameter hyper-space is likely not to be fully explored by the optimisation procedure, we believe that the set of solutions we obtained by repeating the optimisation with various initial guesses is likely to provide a good picture of the possible geometries that lead to efficient injection. Figure 4(a) shows a typical example of such a solution. This geometry has been obtained for a target group velocity of $0.01c$ in the first valence band. The superimposed red curve represents $|E|^2$ as a function of the z -coordinate. The field intensity in the periodic waveguide is roughly 40 times larger than that in the z -invariant waveguide. The optimised injector parameters are given in the figure caption. We note that the five slit widths progressively increase, while the five ridge widths progressively decrease along the injector. This progressive variation is well traditional for tapered mirrors engineered for ultrahigh Q microcavities, and is understood as a progressive transverse-mode-profile matching of the various Bloch modes involved in the tapered geometry [21]. This guarantees small scattering losses, and therefore a high injection efficiency in the present context.

Figure 4(b) shows the injector performance as a function of the frequency of the incident guided mode, or equivalently as a function of the group velocity of the periodic-waveguide Bloch mode. The maximal injection efficiency T (solid black curve) is obtained for $v_g=0.015$ ($\lambda \approx 1.65 \mu\text{m}$) and is $\approx 99.9\%$. As the wavelength deviates from this value, the performance degrades. Actually, it is limited by the back-reflection R (blue circles) that rapidly increases, while the radiation losses $L=1-T-R$ (magenta dashed curve) remain below 10^{-3} over almost the entire spectral range. The 1dB ($T>0.8$) bandwidth is determined to be 275GHz, a value approximately 10 times larger than that achieved with purely periodic injectors in Fig. 3. The broader bandwidth is a net effect of the large number of degrees of freedom that we have intentionally used for the 2D injector. The latter consists in 5 pairs of ridges-slits, while only $m=2$ layer pairs were used for the 1D injector in Fig. 3.

Similar performances have been obtained for smaller group velocities but with smaller bandwidths. For instance, for $v_g=0.002c$, similar computations have shown that efficient injectors with a maximum injection efficiency of 99.4% can be designed with a 20 times smaller bandwidth. We believe that group velocities in the range of 0.01 that corresponds to a slow down factor of ≈ 40 may represent an interesting regime for on-chip optical processing with ≈ 250 GHz bandwidths. Smaller group velocities are likely to offer prohibitively small bandwidths and their associated propagation loss due to various disorders induced by fabrication inaccuracies may additionally be a critical issue [23-25].

4. Conclusion

In periodic media, Bloch modes with small group velocities are interference patterns and in their simplest form are created by the superposition of a forward- and a backward-propagating mode that together form a standing or a slowly-moving mode pattern. When illuminated from a z -invariant medium, light is only weakly coupled into the slow Bloch mode. For bi-layer periodic structures, we have derived closed-form expressions for the coupling efficiencies in the vicinity of the valence and conduction bands. The expressions evidence that the impedance mismatch essentially arises from the standing-wave character of the slow Bloch mode and that the injection efficiency is proportional to the group velocity of the Bloch mode, the proportionality factor being weakly dependant on the actual geometric parameters.

To overpass the impedance-mismatch problem, we have explored a new route for injecting light efficiently into slow Bloch modes. In contrast to previous works using adiabatic tapers that implement a progressive light slowdown through a continuous change of the waveguide geometry, the present injectors rely on interference effects, in a way analogue to the classical multi-film-stack approach used for AR-coating [26] or impedance matching with quarter-wave transformers in the transmission line theory [27]. The net benefit is compactness. For instance, we have shown that very short couplers whose length are scaling as $\log(c/v_g)$, may provide perfect injection (100% coupling efficiency) at a single frequency for arbitrary-small group velocities. For 2D geometries like periodic slab waveguides, we have shown that radiation losses into the cladding are not a critical issue. We rather found that high injection efficiency together with a broadband injection is indeed difficult to manage both together, especially in the slow light regime for $v_g < c/100$. There is a compromise. These conclusions have been reached for Bloch modes in thin-film stacks and in periodic slab waveguides, but are expected to remain quantitatively valid for other kinds of periodic ridge waveguides. Photonic crystal waveguides, like single-row-defect waveguides, deserves a specific study because the physical nature of the light confinement is different especially in the slow light regime. We expect that this prospective study will be helpful for further investigations in the field.

Acknowledgments

This research is partly supported under the European contract SPLASH of the 6th PCRD and by the Agence Nationale de la Recherche under contract MIRAMAN of the French ANR Nano2006. The authors thank C. Sauvan and G. Lecamp for fruitful discussions. P. Velha acknowledges a BDI CNRS-CEA fellowship. He is also at the Laboratoire Silicium Nanoélectronique Photonique et Structure of the CEA/DRFMC and at the Laboratoire des Technologies de la Microélectronique in Grenoble.